

Full title

On the choice between walls and berms for road traffic noise shielding including wind effects

Authors

Timothy VAN RENTERGHEM, Dick BOTTELDOOREN

Affiliation

T. Van Renterghem: Ghent University, Department of Information Technology, Sint Pietersnieuwstraat 41, B- 9000 Gent, Belgium. (timothy.van.renterghem@intec.ugent.be)

D. Botteldooren: Ghent University, Department of Information Technology, Sint Pietersnieuwstraat 41, B- 9000 Gent, Belgium. (dick.botteldooren@intec.ugent.be)

Corresponding Author

T. Van Renterghem: Ghent University, Department of Information Technology, Sint Pietersnieuwstraat 41, B- 9000 Gent, Belgium. (timothy.van.renterghem@intec.ugent.be)

TEL: +32 9 264 36 34 FAX: +32 9 264 99 69

1. Introduction

There is a growing body of evidence for negative health effects caused by continued exposure to road traffic noise. Sleep disturbance, noise annoyance, ischaemic heart diseases, cognitive impairment of children and tinnitus are most often mentioned (Fritschi et al., 2011). Residents of areas close to highways and big arterial roads are amongst the most affected.

A well designed noise barrier is often the only possibility to significantly reduce levels at such highly exposed receivers, and is therefore still a popular noise abatement strategy. Other measures like silent road top covers can be useful (and complimentary), but will not give the noise reduction that can be obtained by barriers at short distance. Furthermore, such road surface top layers typically lose (part of) their positive acoustic effect over time (Sandberg and Ejsmont, 2002). Car engines and tires are subject to continued noise control engineering. This is however a slow process. In addition, it cannot be considered as a measure to tackle an urgent local noise problem. Traffic related measures like reducing speed limits, which might give a reduction in the order of several dBAs, can be mentioned as well. However, such a measure might conflict with the basic functionality of a high-speed road. Façade insulation might tackle specific noise-related problems such as sleep disturbance. It has been shown, however, that noise annoyance is not reduced as much as could be expected on the basis of level reduction by increased façade insulation (Miedema and Borst, 2007). This can be explained by the fact that people open windows and spend time outside their dwellings.

The choice between an earth berm (also called earth mound or bund) and a noise wall often needs to be made in a planning phase. Both reduce noise levels by preventing direct sound propagation between source and receiver, forcing sound to diffract around the barrier edges, leading to a decreased intensity. Major parameters influencing the acoustic shielding are the height of the noise barrier, the position of source and receiver, and the design and acoustic properties of the barrier top (e.g. Hothersall et al., 1991; Ishizuka and Fujiwara, 2004; Monazzam and Lam, 2005; Watts and Morgan, 1996). Given that complex interactions occur between the different contributions towards a shielded receiver and the soil on which the barrier is placed, the properties of the latter are important (e.g. Hutchins et al., 1984a; Isei et al., 1980; Jonasson, 1972).

The acoustic efficiency (in a windless, homogenous atmosphere) of both berms and walls was compared in detail by scale modeling of a typical highway setup (Busch et al., 2003). The top height of both the berms and walls compared in that study was fixed at 4 m. The optimal choice was shown to depend on the acoustical properties of the constituting material of the berm. In case packed earth was modelled, a noise wall reduced total A-weighted road traffic noise levels more than the berm. When an acoustically softer berm was modeled, the noise reduction of the berm increased sufficiently to favor berms by about 2 dBA. Decreasing the berm slope was shown to increase shielding in case of the acoustically soft berm only. For the packed earth berms, slope angle was not an important parameter. Earlier work showed the need to make earth berms typically somewhat higher compared to walls to yield similar shielding. This is caused by the fact that the wall top position can be placed closer to the noise source (or to the receiver), which is more efficient (see e.g. Kotzen and English, 2009). This lower shielding can however be compensated by placing a small screen on top of the berm, or by constructing berms with flat tops (Hutchins et al., 1984b).

The efficiency of noise walls is largely reduced for downwind receivers (e.g. De Jong and Stusnick, 1976; Rasmussen and Arranz, 1998; Salomons, 1999). The typical flow field near a vertically erected wall results in large vertical gradients in the horizontal component of the wind velocity just above the barrier top, leading to downward refraction of sound. At close distance, diffracted sound is bent downwards and enters the (deep) shadow zone formed by the barrier. Since more sound energy reaches this zone, the shielding efficiency decreases compared to a windless atmosphere. At larger distance, sound rays shearing over the barrier top (without interacting with the barrier) can be bent downward as well to reach the zone shielded by the barrier. The latter effect also occurs in open field in absence of a barrier. While at close distance refraction is mainly caused by the action of wind, at larger distance both downwind and temperature inversion conditions can lead to downward refraction.

Negative wind effects near noise walls can be reduced by placing a row of trees, acting as a windbreak, behind the barrier. This has been shown by means of a wind tunnel experiment at scale (Van Renterghem and Botteldooren, 2003a; Van Renterghem et al., 2002), a measurement campaign along a highway (Van Renterghem and Botteldooren, 2002), and by means of detailed numerical calculations (Van Renterghem and Botteldooren, 2003, 2008).

In contrast to noise walls, berms are aerodynamically smoother, and therefore the screen-induced refraction of sound by wind could be weaker. So when comparing the efficiency of a noise berm and a wall, including wind effects is necessary. This is the scope of this paper. Note that highway noise barriers are most often located in open fields, so wind shelter from surrounding objects is limited, and large wind speeds might be impinging on the barrier.

During planning, there are clearly some relevant non-acoustical aspects as well. An earth berm can be rather easily integrated in the landscape and preserves the feeling of “openness” (Kotzen and English, 2009). Furthermore, berms can be vegetated and can therefore be considered as fully green noise reducing measures. Classical noise walls, on the other hand, are often perceived as intruding in the rural landscape. Noise walls can be “greened” to some extent, either by adding substrates to grow (small) vegetation, or by using recycled materials, of which many examples can be found in the book by Kotzen and English (2009). Other advantages of berms are that safety fences are not needed, the unlimited life span, the absence of issues related to graffiti, and the lower cost if excess material from other locations can be used (Kotzen and English, 2009). A drawback of an earth berm, which is typically wedge-shaped, is the need for a larger basal area compared to a noise wall.

The responses of residents near a newly constructed noise barrier can be highly polarized. The study reported by Bendtsen (1994) concludes that the previous high noise levels are quickly forgotten, while dissatisfaction with the loss of view remains. Another study (Nilsson and Berglund, 2006) states that the net public reaction to highway noise barriers is positive, although specific reactions can vary strongly. The social survey conducted by Arenas (2008) rank loss of sunlight, restriction of view/visual impact, and restricted access to the other side as major drawbacks for dwellings within 100 m distance from a newly built 3-m high noise wall. These findings shows that visual aspects related to noise barriers are clearly important.

In this study, noise walls and a number of berms will be numerically evaluated, with focus on downwind sound propagation. Planning based on such a worst-case scenario can be considered as good practice. This paper does not aim at developing new calculation methods. A previously

developed and validated hybrid two-dimensional full-wave sound propagation model (FDTD-PE) (Van Renterghem et al., 2005), combined with a commercial computational fluid dynamics (CFD) software (“Fluent”, 2006), will be used. Some general background information concerning the modeling approaches will nevertheless be provided. The same calculation procedure was applied to study the effect of tree canopy shape near noise walls in wind (Van Renterghem and Botteldooren, 2008).

2. Numerical model

2.1. Wind fields

The wind velocity fields near the noise barriers were calculated with the CFD software Fluent 6.3 (“Fluent”, 2006). The Reynolds-averaged Navier-Stokes equations were solved by applying a standard k-ε “turbulence closure” model. The latter is a common engineering approach to simulate high Reynolds number flows as appear near large flow disturbing structures like noise barriers along highways. The outcomes of the flow model are the horizontal u_x and vertical u_z components of the wind velocity. Appropriate boundary conditions were applied, assuming a neutral, atmospheric boundary layer in equilibrium (Richards and Hoxey, 1993). The vertical (inflow) profile of the horizontal wind velocity u_x under this condition reads:

$$u_x = \frac{u_*}{\kappa} \ln \left(1 + \frac{z}{z_0} \right)$$

where u^* is the friction velocity, κ is the Von Karman constant (equal to 0.4 for air), z is the height above ground level, and z_0 is the aerodynamic roughness length. The flow simulations were performed for friction velocities of 0.4 m/s and 0.8 m/s, and an aerodynamic roughness length of 0.01 m was used. These values correspond to a wind speed of 6.9 m/s and 13.8 m/s at a height of 10 m, respectively.

2.2. Sound propagation model

Sound propagation between source and receivers was calculated with the Finite-Difference Time-Domain (FDTD) model, coupled to the Greens Function Parabolic Equation (GFPE) method. This 2D-hybrid model was shown to be computationally very efficient, without resulting in loss of accuracy (Van Renterghem et al., 2005). The effect on sound propagation of complex flow fields near source and barriers is accurately taken into account by the computationally demanding FDTD method. At the same time, the computational efficiency of the GFPE model is exploited to assess the barrier efficiency at longer distance, still taking into account refraction. The different regions of the simulation domain, with the corresponding numerical methods, are shown in Fig. 1.

The FDTD method is used for solving the moving-medium sound propagation equations (Blumrich and Heimann, 2002; Ostashev et al. 2005; Van Renterghem and Botteldooren, 2003b) in the direct vicinity of the noise barriers. The stationary flow field as calculated by the flow model was used as a background flow. This implies that refraction of sound by wind is accounted for accurately. The effect of upward flow appearing close to the barriers is included as well. The optimal numerical discretisation scheme depends on whether wind is present or not. In absence of flow, the efficient staggered spatial and staggered temporal grid (Botteldooren, 1995)

was used. In wind, staggered-in-space calculations were combined with the prediction-step staggered-in-time (PSIT) approach (Van Renterghem and Botteldooren, 2003b, 2007). The Zwicker and Kosten model (Zwicker and Kosten, 1949) was used to account for the interaction between sound waves and natural soil. The latter was explicitly included in the simulation domain as a second propagation medium. A discussion on the use of this model in the FDTD context can be found in the work by Salomons et al. (2002) and by Van Renterghem and Botteldooren (2003b). The FDTD method has been validated thoroughly by comparison with measurements, analytical solutions and other numerical methods in outdoor sound propagation applications (Blumrich and Heimann, 2002; Liu and Albert, 2006; Ostashev et al., 2005; Van Renterghem and Botteldooren, 2003b). Of particular interest for the current application is the good agreement between measurements and simulations that was obtained with a coupled CFD-FDTD model for including complex flow near noise walls (Van Renterghem and Botteldooren, 2003b).

The Green's Function PE (GFPE) method (Gilbert and Di, 1993; Salomons, 1998) calculated sound propagation starting at close distance downwind from the noise barrier towards the receiver zone. The GFPE calculation starts from frequency dependent complex pressures on a vertical line, obtained from the FDTD calculations. Refraction is modeled using the effective sound speed approach. Only horizontal flow with range-dependent wind speed profiles is included in this zone. This approximation is justified since the vertical component of the flow field is very limited here.

Turbulent scattering is not considered in this numerical study. Simulations showed that the time-averaged effect of screen-induced turbulent scattering in the shielded region behind a barrier is very limited (about 0.2 dB for a single sound frequency of 500 Hz) in case of downwind sound propagation (Heimann and Blumrich, 2004). This finding was confirmed by calculations by Salomons (2001), showing that the additional effect of turbulence in case of downwind sound propagation over (unscreened) finite-impedance ground is limited. Similarly, the effect of including turbulent scattering in case of downwind sound propagation towards shielded city canyons in an urban environment did not significantly increase levels (Van Renterghem et al., 2006). It can therefore be concluded that turbulence does not need to be considered for studying downwind propagation of broadband noise over a barrier.

2.3. Simulation parameters and setup

The maximum height of the noise barriers considered in this numerical study equals 4 m. Similarly to the cases considered by Busch et al. (2003), the top position of both the walls and berms is fixed. The noise wall considered has a thickness of 0.2 m, and is fully rigid (wall a). Symmetric wedge-shaped berms with slopes 1:1 (berm 1), 1:2 (berm 3) and 1:3 (berm 5) are considered. Consequently, the berm base thicknesses are 8 m, 16 m and 32 m, respectively. Two cases with a flat berm top and slopes of 1:1 and 1:2 are included in the comparison. In the first case (berm 2), a top width of 2 m is assumed, in the second case a top width of 4 m (berm 4). This means that the berm base thicknesses are 10 m and 20 m, respectively. An overview of the wall and berm geometries is shown in Fig. 2.

The fixed-top-position approach could be questioned as already indicated in the introduction of this paper. Good practice suggests placing the wall as close as possible to the source. Additional

calculations were therefore included where a noise wall was placed at the same position as the start of the base of berm 5. This corresponds to a shift of the wall of 12 m towards the source (wall b).

The source (at $x=0$ m) is positioned at 24 m horizontal distance from the top of wall *a* and the berms. To limit the computational cost, a single source height of 0.3 m has been considered as an approximation. The interface between the FDTD and PE model is located at $x=40$ m.

Three receiver zones are considered. The first two zones are at typical ear heights (between $z=1$ m and $z=2$ m), either closely behind the barrier, from $x=50$ m to $x=100$ m (receiver zone 1), or from $x=50$ m to $x=250$ m (receiver zone 2). A third receiver zones also includes receivers at higher elevation (from $z=1$ m to $z=10$ m, and from $x=50$ m to $x=250$ m), and could be used to evaluate the global efficiency, including receivers at different floors of buildings.

Below the source, the acoustically rigid road (e.g. concrete top layer) extends 8 m towards the berm. Grassland is modeled throughout the rest of the simulation zone. In case of berm 5, 4 m of grassland is still present in front of the berm. In case of wall *a*, this zone with grassland in front of the screen extends to 16 m. The Zwicker and Kosten model (Zwicker and Kosten, 1949) was used to model the interaction between sound waves and natural soils in both the FDTD and PE sound propagation domain. Two variants of berm soil are considered, namely grassland and a forest floor. The parameter choices for the Zwicker and Kosten model were based on the large set of fits to measurements as described in the study of Attenborough et al. (2011). For grassland, 26 sites were considered and fitting resulted in an average flow resistivity of 300 kPas/m^2 , a porosity of 0.75, and a structure constant equal to 1. A forest floor is the acoustically soft soil that typically develops under vegetation. A flow resistivity of 20 kPas/m^2 , a porosity of 0.5, and a structure constant of 1.25 were chosen for this type of soil. Including the effect of vegetation itself on the berm is beyond the scope of this study.

The main interest in this study is shielded road traffic noise. Therefore, calculations were limited up to the 1/3 octave band with a centre frequency equal to 1600 Hz. To calculate the energetically averaged sound pressure level in each 1/3 octave band, 20 sound frequencies were considered. The Harmonoise/Imagine road traffic source power model described e.g. in the work of Jonasson (2007) is used to combine the 1/3-octave band levels to total A-weighted traffic noise levels. Source powers depend on vehicle speed and vehicle types. Light vehicles (e.g. a passenger car, category 1) and heavy vehicles (e.g. a truck, category 3) are considered in this study. Some examples of source power spectra (combined rolling and engine noise) are presented in Fig. 3. With increasing vehicle speed, the higher frequency components become more dominant, especially in case of light vehicles.

The following computational parameters were used. The FDTD spatial discretisation step was 0.02 m in both dimensions. This leads to 9.5 computational cells per wavelength for the highest sound frequency considered in this study, which is very close to the rule-of-thumb value of 10 (for a sound speed of 340 m/s). The temporal discretisation step was 40 μs , and 5000 time steps were sufficient to build the GFPE starting fields. For the GFPE calculations, 10 computational cells per wavelength were used in vertical direction. The horizontal propagation step was equal to a single wavelength, in order to have sufficient spatial resolution when plotting sound pressure fields and to accurately account for the rapid changes of the wind speed profiles in the lee of the barrier. At each propagation step, the wind speed profile was updated.

3. Results

Numerical results are presented as spatially averaged insertion losses. The insertion loss is defined as the sound pressure level in absence of a noise barrier in a still atmosphere, minus the sound pressure level in a particular case, defined by berm shape (or wall), berm soil type and downwind wind speed. All other parameters like source-receiver positions, and ground impedances remain unchanged. A positive insertion loss indicates that a berm or wall is effective in shielding noise. Results are summarized in Table 1 for light vehicles and Table 2 for heavy vehicles as total A-weighted road traffic noise insertion losses at different vehicle speeds, averaged over one of the three receiver zones defined above. The insertion losses at corresponding locations were first calculated, before linearly and spatially averaging.

3.1. In absence of wind

The predicted light-vehicle insertion losses for the noise wall (wall a, see Fig. 2) range from 6.5 dBA to 10.2 dBA for speeds ranging from 30 km/h to 130 km/h in receiver zone 1. The values in receiver zone 2 are 5.6 dBA and 7.7 dBA, respectively. In zone 3, values are very close to the ones in zone 1. This speed dependence can be explained by the fact that better shielded high frequencies contribute more to the overall A-weighted sound pressure level as light vehicle speed increases. The heavy-vehicle insertion losses show a smaller dependence on vehicle speed. There is typically a somewhat higher insertion loss at very low speeds compared to light vehicles. At the highest vehicle speeds considered, the insertion loss is again somewhat lower.

Bringing the wall closer to the source (wall b, see Fig. 2) results in an improvement which is more pronounced at the higher vehicle speeds. These improvements range from 0.7 dBA to 4.1 dBA, depending on the vehicle type, vehicle speed and receiver zone considered.

At low vehicle speeds, the berms perform worse than the wall, certainly when comparing with the shifted wall b. At the highest vehicle speeds, the soft berms perform more or less similar to the screen with the same top position, especially the ones with a flat top. Compared to the shifted wall, the performance is however still lower.

The soil cover of the berms plays an important role. The forest-floor berms outperform the grass-covered berms, that are in turn better than the fully rigid ones (results not shown). The importance of soil cover on berms was also identified in the work by Busch et al. (2003). The effect of soil cover depends on vehicle speed and slope angle. For the 1:1-sloped berm (berm 1), the difference between forest floor and grass-cover ranges from 0.9 to 1.4 dBA, for the 1:2-sloped berm (berm 3) from 1.2 to 1.8 dBA, and for the 1:3-sloped berms (berm 5) from 1.6 to 2.7 dBA in receiver zone 1 for light vehicles. Additional calculation showed that in case of a fully rigid berm, the difference between rigid and forest-floor berms might be as large as 5 dBA. This effect can be explained by the larger interaction path between sound waves shearing over the berm in case of the less steep berm slopes and the fact that higher frequencies (higher vehicle speeds) are more affected by differences in soil type. Similar dependence on berm soil is predicted in the other receiver zones. In case of heavy vehicles, the difference between the soil covers considered is somewhat more pronounced than for light vehicles.

The flat-top berms (berm 2 and 4) give a somewhat increased insertion loss compared to the wedges (berms 1, 3, and 5). This is consistent with earlier findings reported in the work of Hutchins et al. (1984b) and Busch et al. (2003). The differences amount up to 1.7 dBA when comparing berm 4 to berm 3 at 130 km/h (both vehicle types, all receiver zones). For these flat-top berms, the importance of soil cover is very similar as for the wedges in all receiver zones.

3.2. Presence of wind

At close distance (receiver zone 1), the wall efficiency decreases strongly with increasing incident wind speed. Pronounced vertical gradients in the horizontal component of the wind speed appear in a large zone downwind from the noise barrier, as shown in Fig. 4. For light vehicles in absence of wind, the averaged insertion losses range from 6.5 dBA to 10.2 dBA for vehicle speeds between 30 km/h and 130 km/h. For an incident wind speed with a friction velocity $u^*=0.4$ m/s, these values reduce to 4.1 dBA and 6.4 dBA, respectively. For the strong wind ($u^*=0.8$ m/s) only 1.6 dBA to 0.6 dBA of the insertion loss remains.

The wind effect is defined as the sound pressure level behind the noise barrier in wind, minus the sound pressure level behind the noise barrier in absence of wind. Positive values indicate a decreased shielding. The wind effect depends weakly on vehicle speed for $u^*=0.4$ m/s for the wall in receiver zone 1, and this dependence is much stronger for $u^*=0.8$ m/s. In case of the shifted screen, the wind effect is even higher, and can be close to 11 dBA in case of $u^*=0.8$ for light vehicles in zone 1. For heavy vehicles, the wind effect is typically somewhat more pronounced. The contour plots in Fig. 5 show that wind makes the insertion loss more spatially dependent compared to the windless situation. This is also illustrated by the larger values for the standard deviations as found in Table 1 and 2 in presence of wind. The insertion loss spectra at a specific receiver point ($x=100$ m, $z=4$ m) are shown in Fig. 6 (wall a), in absence of wind, and in case of moderate and strong winds. The effect of the wind seems to be most prominent at sound frequencies above 100 Hz, and shifts in insertion loss peaks are observed.

In receiver zone 2, the magnitudes of the wind effects at $u^*=0.4$ m/s and $u^*=0.8$ m/s are similar. In some cases, the wind effect at the lower wind speed can even be higher than at the higher wind speed. Averaged wind effects are higher in receiver zone 3 than in receiver zone 1 for the lower wind speed. The insertion losses in receiver zone 3 become almost independent of vehicle speed in case of light vehicles. For heavy vehicles, the averaged insertion loss of screen a is reduced to 1 dBA ($u^*=0.4$ m/s) and 0.4 dBA ($u^*=0.8$ m/s) at a vehicle speed of 70 km/h. For the shifted screen b, these values are about 0.2-0.3 dBA higher.

The effects observed in receiver zone 2 can be explained as follows. With increasing wind speed, vertical gradients in its horizontal component, the driving forces for refraction of sound by wind, become larger and therefore a lower shielding could be expected behind the noise barrier. This is what is observed at close distance behind the barrier in receiver zone 1. However, as mentioned in the introduction, the soil on which the noise barrier is placed is important as well for the assessment of the global screen efficiency. In case of strong refraction and when a larger area downwind is included like in receiver zone 2, this could lead to an increased number of interactions between sound waves and the absorbing (grass) soil. Salomons (2001) illustrates these “multiple bounce effects” using ray tracing. As a result, part of the wind effect is counteracted by soil absorption and interfering rays. In zone 3, receivers appear at heights between 1 m and 10 m. At larger heights, soil effects are less pronounced (see e.g. “ISO9613-2”,

1996) and the expected wind speed dependence is observed again. The larger wind effect in this zone compared to receiver zone 1 (especially for the low wind speed) is caused by the fact that a much larger portion of the refracted sound energy is captured by the defined receivers, which is not the case in receiver zone 1 which has a more limited spatial extent. The above mentioned effects could however be partly hidden by complex shifts in interference patterns induced by the local flow.

Also the steepest berm (berm 1) is largely affected by the action of wind as illustrated by the field plots in Fig. 4. In receiver zone 1 and for the low wind speed, similar effects as for wall a are observed. For the higher wind speed, wind effects are however somewhat more moderate than for the wall. In receiver zone 2, wind effects are lower than in zone 1 for the higher wind speed, and the dependence of wind speed seems smaller there as was the case for the noise wall.

The wind effect decreases with decreasing berm slope angle. For berm 3 (with a 1:2 slope), the light-vehicle wind effect is at maximum 1.8 dBA ($u^*=0.4$ m/s) and 3.3 dBA ($u^*=0.8$ m/s) for the forest-floor berm in receiver zone 1, and 1.4 and 2.3 dBA for the grass-covered berm. The negative effect of wind is nearly absent in case of the 1:3-sloped berm (berm 5), with a median value for the wind effect of only 0.9 dBA in all receiver zones (for both grass-covered and forest-floor berms, and for both heavy and light vehicles). The reason for this is that only at the lee side of the berm, very close to its surface, strong downward refracting gradients appear (see Fig. 4). For the grass-covered berm at a vehicle speed of 130 km/h, almost no wind effect (< 0.3 dBA) is observed in receiver zone 1 at both wind speeds considered in this analysis. When looking at the overall road traffic noise insertion loss, berm 5 (forest floor, light vehicles) still gives 8.3 dBA on average under strong wind conditions for a vehicle speed of 130 km/h (instead of 9.0 dBA in absence of wind, receiver zone 1), while the wall efficiency was only 0.6 dBA (instead of 10.2 dBA in absence of wind, receiver zone 1, wall a). This is also illustrated by the contour plots in Fig. 5 allowing a detailed comparison of the spatially dependent insertion loss in case of berm 5 in the absence and presence of wind. The insertion loss spectra at a specific receiver point ($x=100$ m, $z=4$ m) are shown in Fig. 7 (berm 5, forest floor), in absence of wind, and in case of moderate and strong winds. The main effect of the wind seems to be a shift in insertion loss peaks, which only slightly affects the total road traffic noise shielding.

For the shallow berms, the importance of soil cover was identified earlier. A grass-covered 1:3-sloped berm gives about 6.2 dBA (light vehicle, 130 km/h, receiver zone 1) independent of wind speed, and also outperforms a wall under strong wind. In receiver zone 3, berm 5 (forest floor) gives an improvement of 6.8 dBA for light vehicles compared to a straight wall ($u^*=0.4$ m/s, 130 km/h, wall a). Only in receiver zone 2, this better performance of the berm in wind compared to wall a is more moderate.

The berms with a flattened top are less negatively affected by the action of the wind. Berm 2 gives a maximum wind effect of 4.6 dBA, while berm 1 with similar slope angles give a maximum wind effect of 8.6 dBA (over all receiver zones, vehicle speeds, vehicle types, and soil types considered). Note that in absence of wind, the insertion loss was already higher for berm 2 than for berm 1 in all cases. For berm 4, wind effects are limited and are smaller than 1 dBA for most parameter combinations in receiver zone 1 and 3 for the low wind speed; in receiver zone 3 the maximum observed effect equals 1.7 dBA. For the higher wind speed, most wind effects are below 2 dBA in all receiver zones. Wind effects near berm 4 are lower than near berm 3, which is clearly illustrated by comparing the wind velocity gradient field plots in Fig. 4.

Berm 4 with a forest floor yields the best shielding under strong wind for vehicle speeds above 70 km/h for both light and heavy vehicles in all receiver zones. For lower vehicle speeds in zone 2, berm 2 is slightly better for both vehicle types. In zone 1, berm 4 gives the largest insertion loss also at the lower vehicle speeds. Berm 4 (and berm 2) screen noise significantly better than the 4-m high wall in all receiver zones, and for all vehicle speeds and vehicle types considered, under strong wind.

Significant interactions between the soil cover of the berm and the action of wind seem absent in the three receiver zones. Wind effects do not depend on the soil cover on the berm. Only for the steepest berm (berm 1), a small dependence could be observed, showing somewhat less pronounced wind effects for the acoustically harder berms.

The wind effects for heavy vehicle noise follow very similar trends as for light vehicles and are also similar in magnitude. For berm 5, the wind effect could even be slightly negative in receiver zones 1, indicating an increase in insertion loss by the action of the wind.

4. Discussion and conclusions

In this study, a comparison is made between the road traffic noise shielding provided by 4-m high walls and berms. Downwind sound propagation is focused on which is a worst-case scenario for noise barrier shielding. A previously developed and validated full-wave numerical sound propagation model was used. The results show that in a homogeneous and still atmosphere, a noise screen is preferred when assuming that the wall can be placed at the foot of the berm at the source side. In case the same top position for both the wall and berm are used, an acoustically soft berm (e.g. covered with a typical soil as develops under vegetation) with a flat top gives similar shielding as the wall. With decreasing (inner) slope angle, the acoustic impedance of the berm becomes more important. In case of wind, the noise wall efficiency largely decreases. Strong wind might lead to a nearly complete loss of any shielding relative to sound propagation over unobstructed terrain in absence of wind. In contrast, with decreasing berm slope angle, the (negative) action of the wind decreases significantly. The vertical gradients in the horizontal component of the wind field are largely decreased compared to gradients near vertically erected walls. For berms with a slope of 1:3, or steeper slopes with a flat top, the averaged wind effect can be smaller than 1 dBA in many cases.

When looking at long-term equivalent noise levels, the periods with downwind sound propagation are often determining. This statement forms the basis of the calculation of long-term averaged noise level in e.g. the ISO 9613-2 model ("ISO 9613-2", 1996). Periods with upwind sound propagation are assumed not to contribute to these long-term equivalent levels, especially for sources and receivers close to the ground surface ("ISO 9613-2", 1996). Furthermore, the measurement campaign described in the study of Van Renterghem and Botteldooren (2002) showed that the downwind effect behind a noise wall is not strictly limited to the periods where the wind is blowing exactly normal to the wall. Similar effects are observed for deviations of ± 45 degrees relative to the normal on the wall.

The local wind direction and wind speed distribution, and orientation of the noise barrier should therefore be considered for a long-term performance assessment. As an example, a comparison between wall b and berm 4 is made. When assuming that the wind direction is uniformly distributed, downwind conditions, following the findings in the work by Van Renterghem and

Botteldooren (2002), appear 25 % of the time. Similarly, assume that the upwind sound propagation condition is present 25 % of the time as well. In the remaining 50 %, there is no clear downwind or upwind condition, and the windless insertion loss will be taken for these periods. This leads to a global predicted berm efficiency of 11.1 dBA (assuming $u^*=0.4$ m/s in case of downwind sound propagation) and 10.8 dBA ($u^*=0.8$ m/s) for a light vehicle at 100 km/h in receiver zone 3 (heights between 1 m and 10 m, distances between 50 m and 250 m from the source). For the wall, the corresponding values are 8.3 dBA and 7.7 dBA, respectively.

As a result, it can be expected that in many situations, non-steep and acoustically soft berms are likely to outperform walls in a long-term assessment. In addition, a non-steep berm will limit sound reflection on its source side. Reflected sound could potentially reach receivers at the non-shielded side of the source. For walls, such reflections can also be reduced by making the surface of the noise wall absorbing, however, at an increased cost. The positive non-acoustic parameters related to natural berms can be strong arguments as well in this discussion, certainly in case of non-steep ones. Less severe slopes look more natural and are easily planted, while maintaining a stronger feeling of openness and might be unrecognizable as a noise barrier in the landscape in time (Kotzen and English, 2009). Ecological impacts (see e.g. Arenas, 2008) like wildlife habitat fragmentation and bird strikes are expected to be less pronounced near (non-steep) earth berms compared to lengthy, vertically erected (transparent) barriers. In addition, natural berms could be positive from a psycho-acoustical point of view as well. It was found that road traffic noise perception is influenced by visual stimuli, and with an increasing degree of urbanization, the perception becomes less pleasant (Viollon et al., 2002). The main drawback for (non-steep) berms is that they are more land-taking. It can therefore be concluded that non-steep berms are preferred, both from a landscape and acoustical point of view.

In this numerical study, two-dimensional sound propagation calculations were performed, implying a coherent line source, and infinitely long noise barriers with constant cross-sections. This approach is justified by the already very large computational cost in solving the complex, coupled flow and sound propagation problem. In addition, no other methods are available that can handle all aspects considered here in such an extended simulation area, still covering a sufficient part of the road traffic noise frequency spectrum. Road traffic is however more accurately described by an incoherent line source since it is generated by independent vehicles. When looking at noise barrier efficiency at individual frequencies, significant differences are observed when comparing calculations made by these two types of line sources (Duhamel, 1996; Jean et al., 1999). When averaging to total A-weighted road traffic noise levels, differences become much smaller. Typically, the coherent line source insertion loss slightly overpredicts shielding, mainly at low receiver heights (Jean et al., 1999). In this study, the same calculation approach has been used for evaluating both walls and berms, leading to reliable conclusions concerning the optimal choice. Furthermore, relative effects like e.g. the wind effect, or the difference between berm soil cover, will be hardly affected by the choice of source type.

Note that in the calculations presented in this paper, vegetation acting as a windbreak near berms and walls has not been considered. A (dense) row of trees behind a noise wall e.g. was shown to limit the screen-induced refraction of sound by wind (Van Renterghem and Botteldooren, 2002; Van Renterghem and Botteldooren, 2008). Additional scattering of sound inside the acoustic shadow zone might be observed compared to a barrier without trees. Since this is mainly a high-frequency phenomenon, its importance for total A-weighted road traffic noise is limited and

measured to be lower than 1 dBA in absence of wind (Van Renterghem and Botteldooren, 2002). The presence of a row of trees, on the other hand, might lead to an increase in shielding of 4 dBA (Van Renterghem and Botteldooren, 2002) compared to a noise wall without trees in wind.

References

1. Arenas, J., 2008. Potential problems with environmental sound barriers when used in mitigating surface transportation noise. *Science of the total environment* 405, 173-179.
2. Attenborough, K., Bashir, I., Taherzadeh, S., 2011. Outdoor ground impedance models. *Journal of the Acoustical Society of America* 129, 2806-2819.
3. Bendtsen, H., 1994. Visual principles for the design of noise barriers. *Science of the total environment* 146/147, 67-71.
4. Blumrich, R., Heimann, D., 2002. A linearized Eulerian sound propagation model for studies of complex meteorological effects. *Journal of the Acoustical Society of America* 112, 446-455.
5. Botteldooren, D., 1995. Finite-difference time-domain simulation of low-frequency room acoustic problems. *Journal of the Acoustical Society of America* 98, 3302-3308.
6. Busch, T., Hodgson, M., Wakefield, C., 2003. Scale-model study of the effectiveness of highway noise barriers. *Journal of the Acoustical Society of America* 114, 1947-1954.
7. De Jong, R. Stusnick, E., 1976. Scale model studies of the effect of wind on acoustic barrier performance. *Noise Control Engineering* 6, 101-109.
8. Duhamel, D., 1996. Efficient calculation of the three-dimensional sound pressure field around a noise barrier. *Journal of Sound and Vibration* 197, 547-571.
9. Fluent, 2006. *Computational Fluid Dynamics Software*, version 6.3, Fluent, Incorporated, Centerra Resource Park, 10 Cavendish Court, Lebanon, NH 03766.
10. Fritschi, L., Brown, L., Kim, R., Schwela, D., Kephelopoulous, S., 2011. Burden of disease from environmental noise – Quantification of healthy life years lost in Europe, WHO European Centre for Environment and Health, Bonn Office.
11. Gilbert, K., Di, X., 1993. A fast Green's function method for one-way sound propagation in the atmosphere. *Journal of the Acoustical Society of America* 94, 2343-2352.
12. Heimann, D., Blumrich, R., 2004. Time-domain simulations of sound propagation through screen-induced turbulence. *Applied Acoustics* 65, 561-582.
13. Hothersall, D., Crombie, D., Chandler-Wilde, S., 1991. The performance of T-shape profile and associated noise barriers. *Applied Acoustics* 32, 269-81.
14. Hutchins, D., Jones, H., Russell, L., 1984a. Model studies of barrier performance in the presence of ground surfaces. Part I – Thin, perfectly reflecting barriers. *Journal of the Acoustical Society of America* 75, 1807-1816.
15. Hutchins, D., Jones, H., Russell, L., 1984b. Model studies of barrier performance in the presence of ground surfaces. Part II – Different shapes. *Journal of the Acoustical Society of America* 75, 1817-1826.
16. Isei, T., Embleton, T., Piercy, J., 1980. Noise reduction by barriers on finite impedance ground. *Journal of the Acoustical Society of America* 67, 46-58.
17. Ishizuka, T., Fujiwara, K., 2004. Performance of noise barriers with various edge shapes and acoustical conditions. *Applied Acoustics* 65, 125-141.
18. ISO 9613-2 Acoustics – attenuation of sound during propagation outdoors – Part 2. International Organisation for Standardisation, Geneva, Switzerland, 1996.
19. Jean, P., Defrance, J., Gabillet, Y., 1999. The importance of source type on the assessment of noise barriers. *Journal of Sound and Vibration* 226, 201-216.
20. Jonasson, H., 1972. Sound reduction by barriers on the ground. *Journal of Sound and Vibration* 22, 113-126.

21. Jonasson, H., 2007. Acoustical source modelling of road vehicles. *Acta Acustica united with Acustica* 93, 173-184.
22. Liu, L., Albert, D., 2006. Acoustic pulse propagation near a right-angle wall. *Journal of the Acoustical Society of America* 119, 2073-2083.
23. Miedema, H., Borst, H., 2007. Rating environmental noise on the basis of noise maps within the framework of the EU Environmental Noise Directive. *Proceedings of 36th International Congress and Exposition on Noise Control Engineering (INTERNOISE)*, Istanbul, Turkey.
24. Monazzam, M., Lam, Y., 2005. Performance of profiled single noise barriers covered with quadratic residue diffusers. *Applied Acoustics* 66, 709-730.
25. Nilsson M., Berglund, B., 2006. Noise annoyance and activity disturbance before and after the erection of a roadside noise barrier. *Journal of the Acoustical Society of America* 119, 2178-2188.
26. Kotzen, B., English, C., 2009. *Environmental noise barriers – a guide to their acoustic and visual design (second edition)*, Taylor and Francis, London, UK.
27. Ostashev, V., Wilson, D., Liu, L., Aldridge, D., Symons, N., Marlin, D., 2005. Equations for finite-difference, time-domain simulation of sound propagation in moving inhomogeneous media and numerical implementation. *Journal of the Acoustical Society of America* 117, 503–517.
28. Rasmussen, K., Arranz, M., 1998. The insertion loss of screens under the influence of wind. *Journal of the Acoustical Society of America* 104, 2692-2698.
29. Richards, P., Hoxey, R., 1993. Appropriate boundary conditions for computational wind engineering models using the k- ϵ turbulence model. *Journal of wind engineering and industrial aerodynamics* 46-47, 145-153.
30. Salomons, E., 1998. Improved Green's function parabolic equation method for atmospheric sound propagation. *Journal of the Acoustical Society of America* 104, 100-111.
31. Salomons, E., 1999. Reduction of the performance of a noise screen due to screen-induced wind-speed gradients. Numerical computations and wind tunnel experiments. *Journal of the Acoustical Society of America* 105, 2287-2293.
32. Salomons, E., 2001. *Computational atmospheric acoustics*, Kluwer, Dordrecht, The Netherlands.
33. Salomons, E., Blumrich, R., Heimann, D., 2002. Eulerian time-domain model for sound propagation over a finite-impedance ground surface. Comparison with frequency-domain models. *Acta Acustica united with Acustica* 88, 483-492.
34. Sandberg, U., Ejsmont, J., 2002. *Tyre/road noise reference book*, Informex, Kisa, Sweden.
35. Van Renterghem, T., Botteldooren, D., 2002. Effect of a row of trees behind noise barriers in wind. *Acta Acustica united with Acustica* 88, 869-878.
36. Van Renterghem, T., Botteldooren, D., 2003a. Addition to: "Reducing screen-induced refraction of noise barriers in wind with vegetative screens. *Acta Acustica united with Acustica* 89, 381.
37. Van Renterghem, T., Botteldooren, D., 2003b. Numerical simulation of the effect of trees on downwind noise barrier performance. *Acta Acustica united with Acustica* 89, 764-778 (2003).

38. Van Renterghem, T., Botteldooren, D., 2007. Prediction-step staggered-in-time FDTD: an efficient numerical scheme to solve the linearised equations of fluid dynamics in outdoor sound propagation. *Applied Acoustics* 68, 201–216.
39. Van Renterghem, T., Botteldooren, D., 2008. Numerical evaluation of tree canopy shape near noise barriers to improve downwind shielding. *Journal of the Acoustical Society of America* 123, 648-657.
40. Van Renterghem, T., Botteldooren, D., Cornelis, W., Gabriels, D., 2002. Reducing screen-induced refraction of noise barriers in wind by vegetative screens. *Acta Acustica united with Acustica* 88, 231-238.
41. Van Renterghem, T., Salomons, E., Botteldooren, D., 2005. Efficient FDTD-PE model for sound propagation in situations with complex obstacles and wind profiles. *Acta Acustica united with Acustica* 91, 671-679.
42. Van Renterghem, T., Salomons, E., Botteldooren, D., 2006. Parameter study of sound propagation between city canyons with coupled FDTD-PE model. *Applied Acoustics* 67, 487-510.
43. Viollon, S., Lavandier, C., Drake, C., 2002. Influence of visual setting on sound ratings in an urban environment. *Applied Acoustics* 63, 493-511.
44. Watts, G., Morgan, P., 1996. Acoustic performance of an interference-type noise-barrier profile. *Applied Acoustics* 49, 1-16.
45. Zwicker, C., Kosten, C., 1949. *Sound absorbing materials*, Elsevier, New York, USA.

List of table captions

Table 1. Light-vehicle total A-weighted insertion loss (in dBA) for the different cases considered, averaged over the different receiver zones, in function of wind speed and vehicle speed. The values in between brackets are the standard deviations.

Table 2. Heavy-vehicle total A-weighted insertion loss (in dBA) for the different cases considered, averaged over the different receiver zones, in function of wind speed and vehicle speed. The values in between brackets are the standard deviations.

List of tables

Table 1. Light vehicle total A-weighted insertion loss (in dBA) for the different cases considered, averaged over the different receiver zones, in function of wind speed and vehicle speed. The values in between brackets are the standard deviations.

RECEIVER ZONE 1	vehicle speed (km/h)	wall a			wall b			berm1 forest floor			berm1 grass			berm2 forest floor			berm2 grass		
		no wind	u=0.4 m/s	u*=0.8 m/s	no wind	u=0.4 m/s	u*=0.8 m/s	no wind	u=0.4 m/s	u*=0.8 m/s	no wind	u=0.4 m/s	u*=0.8 m/s	no wind	u=0.4 m/s	u*=0.8 m/s	no wind	u=0.4 m/s	u*=0.8 m/s
		30	6.5 (0.6)	4.1 (1.1)	1.6 (1.5)	7.2 (0.4)	4.2 (1)	2 (1.3)	4.5 (0.5)	2.7 (0.7)	1.6 (0.6)	3.6 (0.5)	2 (0.7)	0.9 (0.5)	5.1 (0.5)	4.2 (0.6)	4 (0.5)	4.3 (0.5)	3.3 (0.6)
50	7.1 (0.9)	4.4 (1.5)	1 (2.2)	8.1 (0.8)	4.7 (1.3)	1.3 (2)	5.3 (0.8)	3 (1.2)	1.3 (0.9)	4.3 (0.8)	2.3 (1.1)	0.8 (0.8)	5.9 (0.9)	4.8 (0.9)	4.3 (0.7)	5.1 (0.8)	3.8 (0.9)	3.4 (0.6)	
70	8 (1.2)	5 (1.9)	0.6 (2.8)	9.2 (1.2)	5.3 (1.7)	0.9 (2.7)	6.3 (1.1)	3.5 (1.7)	1.2 (1.3)	5.3 (1.2)	2.9 (1.5)	0.9 (1.2)	7.1 (1.2)	5.7 (1.3)	4.9 (0.9)	6.2 (1.1)	4.6 (1.2)	4 (0.8)	
90	8.9 (1.4)	5.6 (2.3)	0.4 (3.3)	10.3 (1.5)	5.9 (2)	0.7 (3.2)	7.5 (1.4)	4 (2.1)	1.2 (1.5)	6.3 (1.5)	3.5 (1.9)	1 (1.4)	8.4 (1.5)	6.6 (1.5)	5.4 (1.1)	7.4 (1.4)	5.5 (1.5)	4.6 (0.9)	
110	9.6 (1.5)	6.1 (2.5)	0.5 (3.6)	11.2 (1.7)	6.5 (2.2)	0.6 (3.5)	8.4 (1.5)	4.5 (2.3)	1.3 (1.7)	7.2 (1.7)	4 (2.2)	1.2 (1.6)	9.5 (1.6)	7.4 (1.7)	5.9 (1.1)	8.5 (1.5)	6.2 (1.6)	5.2 (1)	
130	10.2 (1.6)	6.4 (2.6)	0.6 (3.7)	11.7 (1.8)	6.9 (2.3)	0.7 (3.6)	9.2 (1.6)	4.9 (2.4)	1.5 (1.8)	7.8 (1.9)	4.5 (2.3)	1.4 (1.7)	10.4 (1.7)	8 (1.7)	6.3 (1.1)	9.3 (1.6)	6.8 (1.7)	5.6 (0.9)	
RECEIVER ZONE 2	vehicle speed (km/h)	wall a			wall b			berm1 forest floor			berm1 grass			berm2 forest floor			berm2 grass		
		no wind	u=0.4 m/s	u*=0.8 m/s	no wind	u=0.4 m/s	u*=0.8 m/s	no wind	u=0.4 m/s	u*=0.8 m/s	no wind	u=0.4 m/s	u*=0.8 m/s	no wind	u=0.4 m/s	u*=0.8 m/s	no wind	u=0.4 m/s	u*=0.8 m/s
		30	5.6 (0.6)	2 (1.5)	2.4 (1.2)	6.6 (0.5)	2.2 (1.4)	1.9 (0.8)	3.8 (0.5)	1.5 (0.9)	2.2 (0.6)	3.1 (0.4)	0.8 (0.8)	1.4 (0.5)	4.3 (0.5)	3 (0.8)	3.5 (0.4)	3.6 (0.5)	2.2 (0.8)
50	5.9 (0.9)	1.2 (2.2)	1.6 (1.4)	6.9 (0.8)	1.7 (2.1)	1.1 (1.2)	4.2 (0.8)	1 (1.4)	1.9 (0.6)	3.4 (0.7)	0.4 (1.3)	1.3 (0.5)	4.7 (0.9)	3.1 (1.2)	3.4 (0.7)	4 (0.8)	2.2 (1.1)	2.6 (0.6)	
70	6.3 (1.2)	0.5 (3.1)	0.8 (1.6)	7.4 (1.3)	1.1 (2.9)	0.2 (1.5)	4.7 (1.1)	0.5 (2)	1.6 (0.7)	3.9 (1)	0.1 (1.9)	1.1 (0.6)	5.3 (1.3)	3.3 (1.6)	3.3 (1.1)	4.5 (1.2)	2.4 (1.6)	2.6 (1)	
90	6.8 (1.5)	0 (3.8)	0.2 (1.8)	8 (1.6)	0.8 (3.6)	-0.5 (1.8)	5.4 (1.4)	0.2 (2.6)	1.3 (0.8)	4.6 (1.3)	-0.1 (2.4)	1 (0.8)	6.1 (1.6)	3.6 (2.1)	3.3 (1.5)	5.3 (1.5)	2.6 (2)	2.7 (1.4)	
110	7.3 (1.7)	-0.3 (4.2)	-0.2 (1.9)	8.5 (1.9)	0.6 (4)	-0.9 (2)	6.1 (1.6)	0.1 (2.9)	1.2 (1)	5.3 (1.5)	-0.1 (2.8)	1.1 (1)	6.9 (1.8)	3.9 (2.4)	3.4 (1.8)	6 (1.7)	3 (2.2)	2.9 (1.7)	
130	7.7 (1.7)	-0.3 (4.5)	-0.4 (2)	8.9 (2)	0.6 (4.3)	-1.1 (2.2)	6.7 (1.7)	0.2 (3.2)	1.3 (1.1)	5.8 (1.6)	0.1 (3)	1.1 (1.1)	7.6 (1.9)	4.3 (2.5)	3.5 (2)	6.7 (1.8)	3.3 (2.4)	3.1 (1.8)	
RECEIVER ZONE 3	vehicle speed (km/h)	wall a			wall b			berm1 forest floor			berm1 grass			berm2 forest floor			berm2 grass		
		no wind	u=0.4 m/s	u*=0.8 m/s	no wind	u=0.4 m/s	u*=0.8 m/s	no wind	u=0.4 m/s	u*=0.8 m/s	no wind	u=0.4 m/s	u*=0.8 m/s	no wind	u=0.4 m/s	u*=0.8 m/s	no wind	u=0.4 m/s	u*=0.8 m/s
		30	6.9 (1.4)	3.4 (1.9)	3 (1.6)	8.2 (1.6)	3.6 (1.9)	3.1 (1.5)	5.3 (1.5)	3.6 (2)	3.8 (1.6)	4.6 (1.5)	3 (2.1)	3.3 (1.7)	5.9 (1.6)	5.4 (2.1)	5.7 (1.8)	5.1 (1.5)	4.5 (2.1)
50	7.8 (1.8)	3 (2.5)	2.9 (2)	9.6 (2.2)	3.3 (2.5)	2.9 (2)	6.4 (1.9)	3.6 (2.5)	4.1 (2)	5.7 (1.9)	3.2 (2.6)	3.7 (2.1)	7.1 (2)	6.1 (2.6)	6.2 (2.3)	6.3 (2)	5.2 (2.5)	5.5 (2.3)	
70	8.8 (2.1)	2.8 (3.1)	2.9 (2.3)	11.1 (2.6)	3.2 (3)	2.7 (2.4)	7.6 (2.2)	3.8 (3)	4.4 (2.3)	6.9 (2.2)	3.6 (3)	4.1 (2.4)	8.5 (2.4)	6.8 (2.9)	6.6 (2.6)	7.6 (2.3)	5.9 (2.9)	6 (2.6)	
90	9.6 (2.3)	2.8 (3.5)	2.8 (2.5)	12.3 (2.9)	3.1 (3.4)	2.5 (2.6)	8.7 (2.4)	4 (3.3)	4.5 (2.5)	8 (2.4)	3.8 (3.3)	4.3 (2.5)	9.7 (2.5)	7.4 (3.1)	6.8 (2.8)	8.7 (2.5)	6.5 (3.1)	6.3 (2.7)	
110	10.2 (2.3)	2.8 (3.7)	2.7 (2.6)	13.2 (3)	3.1 (3.6)	2.3 (2.7)	9.5 (2.5)	4.1 (3.4)	4.5 (2.5)	8.8 (2.4)	4 (3.4)	4.4 (2.6)	10.6 (2.5)	7.8 (3.1)	6.9 (2.8)	9.5 (2.5)	6.8 (3.1)	6.4 (2.8)	
130	10.6 (2.3)	2.8 (3.8)	2.6 (2.7)	13.7 (3.1)	3.1 (3.6)	2.2 (2.8)	10 (2.4)	4.2 (3.4)	4.5 (2.5)	9.3 (2.4)	4.2 (3.4)	4.4 (2.5)	11.2 (2.5)	8 (3.1)	6.9 (2.8)	10.1 (2.4)	7.1 (3.1)	6.5 (2.8)	
RECEIVER ZONE 4	vehicle speed (km/h)	wall a			wall b			berm1 forest floor			berm1 grass			berm2 forest floor			berm2 grass		
		no wind	u=0.4 m/s	u*=0.8 m/s	no wind	u=0.4 m/s	u*=0.8 m/s	no wind	u=0.4 m/s	u*=0.8 m/s	no wind	u=0.4 m/s	u*=0.8 m/s	no wind	u=0.4 m/s	u*=0.8 m/s	no wind	u=0.4 m/s	u*=0.8 m/s
		30	4.3 (1.6)	3.8 (2.3)	4.1 (2.1)	3.2 (1.5)	2.6 (2.2)	2.8 (2.1)	5.2 (1.8)	4.8 (2.2)	4.7 (2.5)	3.9 (1.6)	3.5 (2)	3.3 (2.3)	4.4 (1.6)	4 (2.1)	3.9 (2.5)	2.9 (1.4)	2.5 (2)
50	5.6 (2)	4.7 (2.7)	4.8 (2.5)	4.4 (2)	3.6 (2.7)	3.6 (2.6)	6.5 (2.3)	6.1 (2.7)	5.9 (3)	5.2 (2.1)	4.7 (2.5)	4.4 (2.8)	5.8 (2.1)	5.3 (2.7)	5 (3)	4.2 (1.9)	3.7 (2.5)	3.4 (2.8)	
70	7 (2.4)	5.7 (3.1)	5.4 (2.8)	5.8 (2.4)	4.7 (3.1)	4.5 (2.9)	8.1 (2.7)	7.6 (3.1)	7.1 (3.4)	6.6 (2.5)	6 (2.9)	5.5 (3.2)	7.3 (2.5)	6.7 (3.1)	6.2 (3.4)	5.5 (2.3)	5 (2.8)	4.5 (3.2)	
90	8.2 (2.6)	6.5 (3.2)	5.9 (2.9)	6.9 (2.6)	5.6 (3.2)	5.2 (2.9)	9.6 (2.9)	8.8 (3.3)	8.1 (3.5)	7.9 (2.6)	7.1 (3.1)	6.5 (3.4)	8.6 (2.8)	8 (3.3)	7.3 (3.6)	6.7 (2.5)	6.1 (3)	5.5 (3.4)	
110	9.1 (2.7)	7.1 (3.3)	6.1 (2.9)	7.8 (2.6)	6.2 (3.2)	5.6 (2.9)	10.7 (2.9)	9.8 (3.2)	8.8 (3.5)	8.8 (2.7)	8 (3.1)	7.1 (3.3)	9.6 (2.8)	8.9 (3.3)	8 (3.6)	7.5 (2.6)	6.9 (3)	6.1 (3.3)	
130	9.8 (2.6)	7.4 (3.2)	6.3 (2.9)	8.4 (2.6)	6.6 (3.1)	5.8 (2.8)	11.5 (2.8)	10.5 (3.1)	9.3 (3.4)	9.5 (2.6)	8.5 (3)	7.4 (3.2)	10.3 (2.8)	9.6 (3.2)	8.4 (3.5)	8 (2.6)	7.4 (2.8)	6.5 (3.2)	

Table 2. Heavy vehicle total A-weighted insertion loss (in dBA) for the different cases considered, averaged over the different receiver zones, in function of wind speed and vehicle speed. The values in between brackets are the standard deviations.

RECEIVER ZONE 1	vehicle speed (km/h)	wall a			wall b			berm1 forest floor			berm1 grass			berm2 forest floor			berm2 grass		
		no wind	u*=0.4 m/s	u*=0.8 m/s	no wind	u*=0.4 m/s	u*=0.8 m/s	no wind	u*=0.4 m/s	u*=0.8 m/s	no wind	u*=0.4 m/s	u*=0.8 m/s	no wind	u*=0.4 m/s	u*=0.8 m/s	no wind	u*=0.4 m/s	u*=0.8 m/s
		30	7.4 (0.7)	4.7 (1.3)	1.5 (1.8)	8.2 (0.6)	4.9 (1.2)	2 (1.5)	5.7 (0.6)	3.5 (0.9)	1.9 (0.6)	4.8 (0.7)	2.9 (0.8)	1.5 (0.5)	6.3 (0.7)	5.2 (0.7)	4.8 (0.4)	5.6 (0.7)	4.4 (0.7)
50	7.9 (0.9)	4.8 (1.5)	0.8 (2.2)	9.0 (0.7)	5.1 (1.4)	1.4 (1.9)	6.3 (0.8)	3.7 (1.2)	1.5 (0.8)	5.3 (1)	3.1 (1.1)	1.2 (0.7)	7 (0.9)	5.6 (0.8)	5 (0.3)	6.2 (0.8)	4.7 (0.8)	4 (0.2)	
70	8.5 (1)	5 (1.8)	0.2 (2.6)	9.9 (0.9)	5.4 (1.6)	0.9 (2.2)	7.1 (0.9)	3.8 (1.4)	1.1 (1)	5.9 (1.3)	3.3 (1.3)	0.9 (0.9)	7.9 (1)	6.2 (0.9)	5.2 (0.3)	7.1 (1)	5.2 (0.9)	4.2 (0.2)	
90	9.2 (1.1)	5.2 (2)	-0.2 (2.9)	10.9 (1.1)	5.7 (1.8)	0.5 (2.5)	8 (1)	4.1 (1.7)	0.9 (1.1)	6.5 (1.6)	3.6 (1.5)	0.8 (1)	8.9 (1.2)	6.7 (1)	5.4 (0.3)	8 (1.1)	5.6 (1)	4.4 (0.3)	
110	9.8 (1.1)	5.5 (2.2)	-0.4 (3.1)	11.8 (1.2)	5.9 (1.9)	0.4 (2.7)	8.8 (1.1)	4.3 (1.8)	0.8 (1.3)	7.1 (1.9)	3.9 (1.7)	0.7 (1.1)	9.8 (1.3)	7.2 (1.1)	5.7 (0.4)	8.8 (1.2)	6.1 (1)	4.6 (0.4)	
130	10.2 (1.2)	5.7 (2.3)	-0.4 (3.2)	12.5 (1.3)	6.2 (2)	0.3 (2.8)	9.4 (1.2)	4.5 (1.9)	0.8 (1.3)	7.5 (2.1)	4.1 (1.8)	0.8 (1.2)	10.5 (1.3)	7.6 (1.1)	5.9 (0.5)	9.5 (1.2)	6.4 (1)	4.8 (0.5)	
RECEIVER ZONE 2	vehicle speed (km/h)	wall a			wall b			berm1 forest floor			berm1 grass			berm2 forest floor			berm2 grass		
		no wind	u*=0.4 m/s	u*=0.8 m/s	no wind	u*=0.4 m/s	u*=0.8 m/s	no wind	u*=0.4 m/s	u*=0.8 m/s	no wind	u*=0.4 m/s	u*=0.8 m/s	no wind	u*=0.4 m/s	u*=0.8 m/s	no wind	u*=0.4 m/s	u*=0.8 m/s
		30	4.9 (0.6)	3.8 (0.7)	3.2 (0.5)	3.4 (0.6)	2.4 (0.6)	2 (0.4)	5.7 (0.8)	5.4 (0.8)	5.2 (0.9)	4.3 (0.7)	4 (0.8)	3.9 (0.8)	5 (0.7)	4.6 (0.8)	4.3 (0.9)	2.9 (0.7)	2.6 (0.7)
50	5.6 (0.8)	4.3 (0.8)	3.6 (0.5)	4.1 (0.7)	3 (0.7)	2.4 (0.5)	6.5 (0.9)	6.2 (1)	6 (1)	5 (0.9)	4.7 (0.9)	4.6 (0.9)	5.8 (0.9)	5.4 (1)	5.1 (1)	3.6 (0.8)	3.3 (0.9)	3.2 (0.9)	
70	6.5 (1)	5 (0.9)	3.9 (0.5)	5 (0.9)	3.7 (0.8)	3 (0.5)	7.6 (1.1)	7.2 (1.1)	7 (1.2)	6 (1)	5.6 (1)	5.5 (1.1)	6.8 (1.1)	6.4 (1.1)	6.1 (1.2)	4.4 (1)	4.3 (1)	4.1 (1)	
90	7.6 (1.1)	5.7 (1)	4.4 (0.6)	6 (1)	4.5 (0.8)	3.5 (0.4)	8.8 (1.3)	8.4 (1.3)	8.1 (1.3)	7 (1.1)	6.7 (1.1)	6.5 (1.1)	8 (1.2)	7.6 (1.2)	7.2 (1.3)	5.3 (1.1)	5.3 (1)	5.2 (1)	
110	8.6 (1.2)	6.4 (1)	4.7 (0.6)	6.8 (1)	5.2 (0.8)	4 (0.4)	10 (1.4)	9.6 (1.3)	9.3 (1.3)	8 (1.2)	7.7 (1.1)	7.4 (1.2)	9.1 (1.3)	8.7 (1.3)	8.3 (1.3)	6.1 (1.2)	6.3 (1)	6.2 (1)	
130	9.4 (1.2)	7 (1)	5.1 (0.6)	7.6 (1.1)	5.8 (0.8)	4.4 (0.5)	11 (1.4)	10.6 (1.3)	10.3 (1.3)	8.9 (1.3)	8.5 (1.1)	8.2 (1.2)	10.1 (1.4)	9.8 (1.3)	9.3 (1.4)	6.7 (1.2)	7.1 (0.9)	7 (1)	
RECEIVER ZONE 3	vehicle speed (km/h)	wall a			wall b			berm1 forest floor			berm1 grass			berm2 forest floor			berm2 grass		
		no wind	u*=0.4 m/s	u*=0.8 m/s	no wind	u*=0.4 m/s	u*=0.8 m/s	no wind	u*=0.4 m/s	u*=0.8 m/s	no wind	u*=0.4 m/s	u*=0.8 m/s	no wind	u*=0.4 m/s	u*=0.8 m/s	no wind	u*=0.4 m/s	u*=0.8 m/s
		30	7.1 (1.2)	2.1 (2)	1 (2)	8.9 (1.7)	2.3 (2)	1.2 (1.8)	5.8 (1.3)	2.7 (1.8)	2.3 (1.9)	5.2 (1.3)	2.3 (1.9)	2 (1.9)	6.4 (1.4)	4.9 (1.8)	4.5 (1.8)	5.7 (1.3)	4.1 (1.8)
50	7.5 (1.3)	1.5 (2.5)	0.7 (2.2)	9.8 (1.9)	1.8 (2.4)	0.9 (2.1)	6.4 (1.5)	2.3 (2.2)	2.3 (2.1)	5.7 (1.4)	2 (2.2)	2.1 (2.1)	7 (1.5)	4.9 (2.1)	4.6 (2.1)	6.2 (1.5)	4.1 (2.1)	3.9 (2.1)	
70	7.9 (1.4)	1 (2.9)	0.4 (2.4)	10.7 (2.1)	1.3 (2.8)	0.6 (2.4)	6.9 (1.5)	2 (2.6)	2.3 (2.3)	6.2 (1.5)	1.8 (2.6)	2.1 (2.3)	7.7 (1.6)	5 (2.4)	4.8 (2.4)	6.8 (1.6)	4.1 (2.4)	4 (2.3)	
90	8.2 (1.4)	0.6 (3.3)	0.1 (2.7)	11.6 (2.1)	1 (3.2)	0.3 (2.6)	7.5 (1.5)	1.8 (2.9)	2.2 (2.5)	6.7 (1.5)	1.6 (2.9)	2.1 (2.4)	8.3 (1.6)	5.1 (2.6)	4.8 (2.6)	7.4 (1.6)	4.1 (2.6)	4 (2.5)	
110	8.5 (1.4)	0.3 (3.5)	-0.1 (2.8)	12.3 (2.1)	0.7 (3.4)	0.1 (2.8)	7.9 (1.5)	1.6 (3.1)	2.1 (2.6)	7.1 (1.4)	1.5 (3.1)	2.1 (2.6)	8.8 (1.6)	5.1 (2.7)	4.8 (2.8)	7.8 (1.5)	4.1 (2.7)	4 (2.7)	
130	8.7 (1.3)	0.1 (3.7)	-0.3 (2.9)	12.8 (2)	0.6 (3.6)	-0.1 (2.9)	8.2 (1.4)	1.5 (3.2)	2 (2.7)	7.4 (1.3)	1.4 (3.2)	2 (2.6)	9.1 (1.4)	5 (2.8)	4.7 (2.9)	8.1 (1.4)	4 (2.8)	4 (2.8)	
RECEIVER ZONE 4	vehicle speed (km/h)	wall a			wall b			berm1 forest floor			berm1 grass			berm2 forest floor			berm2 grass		
		no wind	u*=0.4 m/s	u*=0.8 m/s	no wind	u*=0.4 m/s	u*=0.8 m/s	no wind	u*=0.4 m/s	u*=0.8 m/s	no wind	u*=0.4 m/s	u*=0.8 m/s	no wind	u*=0.4 m/s	u*=0.8 m/s	no wind	u*=0.4 m/s	u*=0.8 m/s
		30	5.2 (1.5)	3.9 (2)	3.4 (2)	4 (1.4)	2.7 (1.8)	2.2 (1.9)	6 (1.6)	5.4 (1.9)	4.8 (2.2)	4.7 (1.4)	4 (1.7)	3.3 (2)	5.4 (1.6)	4.7 (1.9)	4.1 (2.3)	3.5 (1.3)	2.9 (1.6)
50	5.9 (1.7)	4.1 (2.3)	3.7 (2.2)	4.6 (1.6)	3 (2.1)	2.7 (2.1)	6.8 (1.9)	6 (2.2)	5.3 (2.5)	5.3 (1.6)	4.5 (2)	3.7 (2.3)	6.1 (1.8)	5.3 (2.2)	4.6 (2.6)	4.2 (1.5)	3.4 (1.8)	2.5 (2.3)	
70	6.6 (1.8)	4.4 (2.5)	3.9 (2.5)	5.3 (1.7)	3.4 (2.4)	3.1 (2.4)	7.7 (2)	6.7 (2.4)	5.8 (2.8)	6.1 (1.7)	5 (2.1)	4.1 (2.6)	7 (1.9)	6 (2.4)	5.1 (2.9)	4.8 (1.6)	3.8 (1.9)	2.9 (2.6)	
90	7.3 (1.8)	4.5 (2.7)	4 (2.7)	5.9 (1.7)	3.6 (2.6)	3.4 (2.6)	8.6 (2)	7.3 (2.4)	6.2 (3)	6.7 (1.7)	5.4 (2.2)	4.4 (2.8)	7.8 (2)	6.6 (2.4)	5.5 (3.1)	5.4 (1.6)	4.2 (2)	3.1 (2.8)	
110	7.8 (1.7)	4.7 (2.8)	4.1 (2.8)	6.4 (1.6)	3.8 (2.7)	3.6 (2.7)	9.3 (1.9)	7.7 (2.4)	6.4 (3.2)	7.3 (1.6)	5.7 (2.2)	4.6 (3)	8.5 (1.9)	7 (2.4)	5.8 (3.2)	5.9 (1.5)	4.5 (2)	3.3 (2.9)	
130	8.3 (1.6)	4.7 (2.9)	4.1 (2.9)	6.8 (1.5)	3.9 (2.7)	3.7 (2.7)	9.8 (1.8)	8.1 (2.4)	6.6 (3.2)	7.7 (1.5)	6 (2.2)	4.7 (3.1)	9.1 (1.8)	7.4 (2.4)	6 (3.3)	6.2 (1.4)	4.7 (1.9)	3.4 (3)	

List of figure captions

Fig. 1. Overview of the simulation areas, indicating the CFD, FDTD and PE region. The 3 receiver zones considered are indicated as well. The axes are not true to scale.

Fig. 2. Overview of the noise barriers that were numerically evaluated in this study. The maximum height is in all cases 4 m. Wall a uses the same top position as the berms; wall b is shifted to the foot of berm 5 in the direction of the source.

Fig. 3. Source power spectra for light and heavy vehicles, at vehicle speeds of 30 km/h and 130 km/h.

Fig. 4. Field plots of the vertical gradients in the horizontal component of the wind velocity near the wall and berms. The incident friction velocity equals $u^*=0.8$ m/s.

Fig. 5. Contour plots of the total A-weighted traffic noise insertion loss for a light vehicle at 100 km/h, for wall a and berm 5 (forest floor), in absence of wind (first row), in case of moderate wind (second row) and in case of strong wind (third rows), in receiver zone 3.

Fig. 6. Insertion loss spectra at a single receiver position ($x=100$ m, $z=4$ m), in absence of wind and in case of moderate and strong winds (wall a).

Fig. 7. Insertion loss spectra at a single receiver position ($x=100$ m, $z=4$ m), in absence of wind and in case of moderate and strong winds (berm 5, with a forest floor).

Figure 1

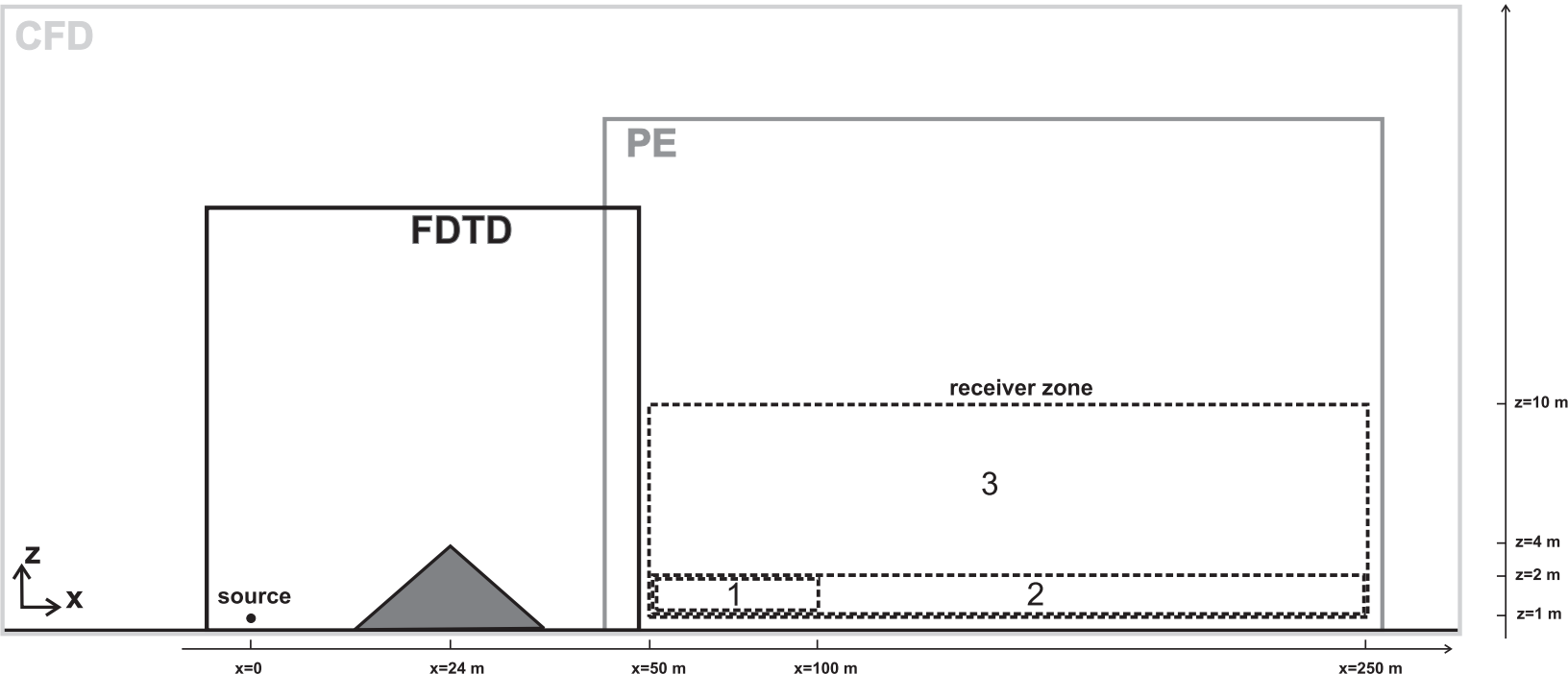


Figure 2

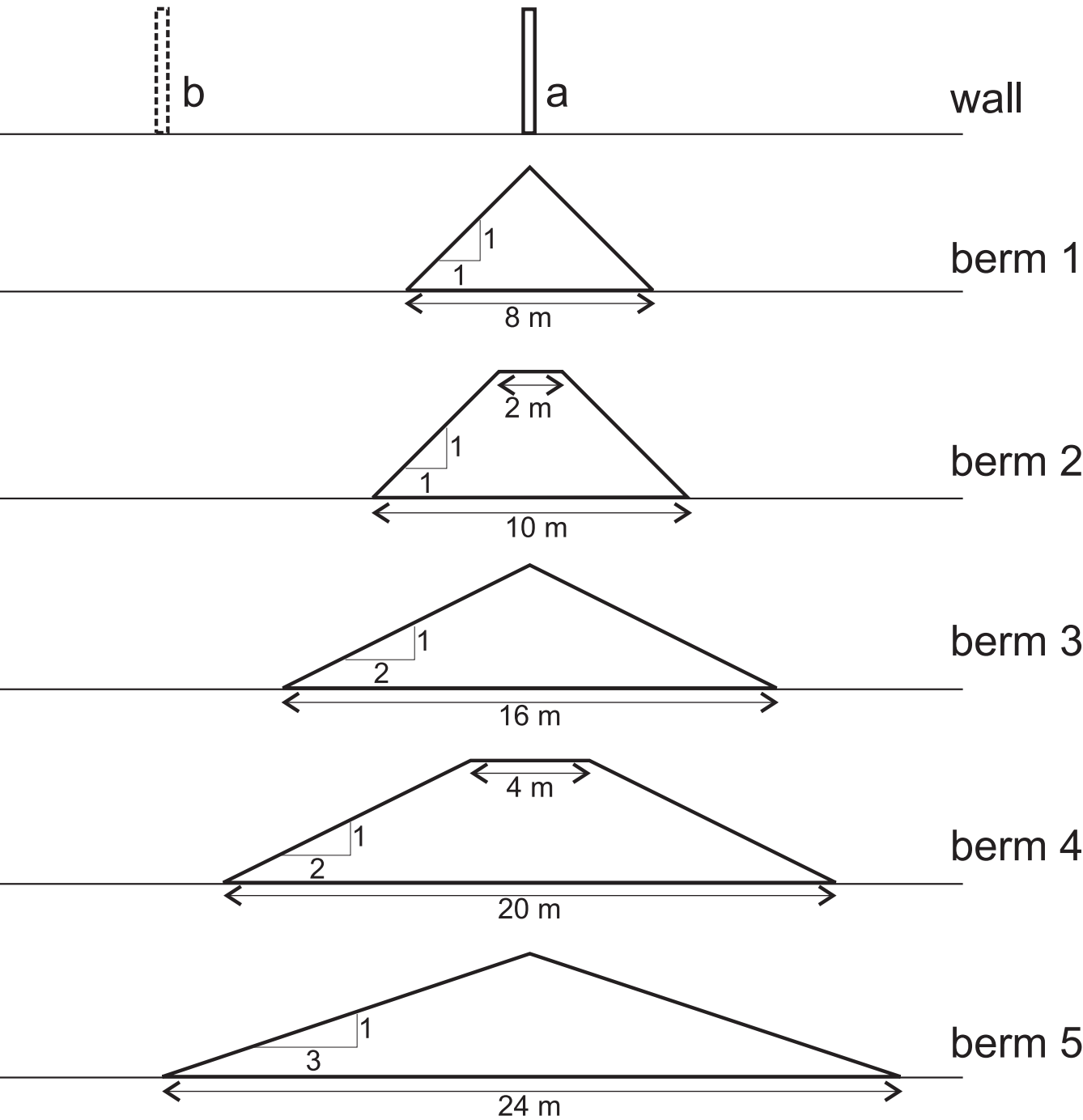


Figure 3

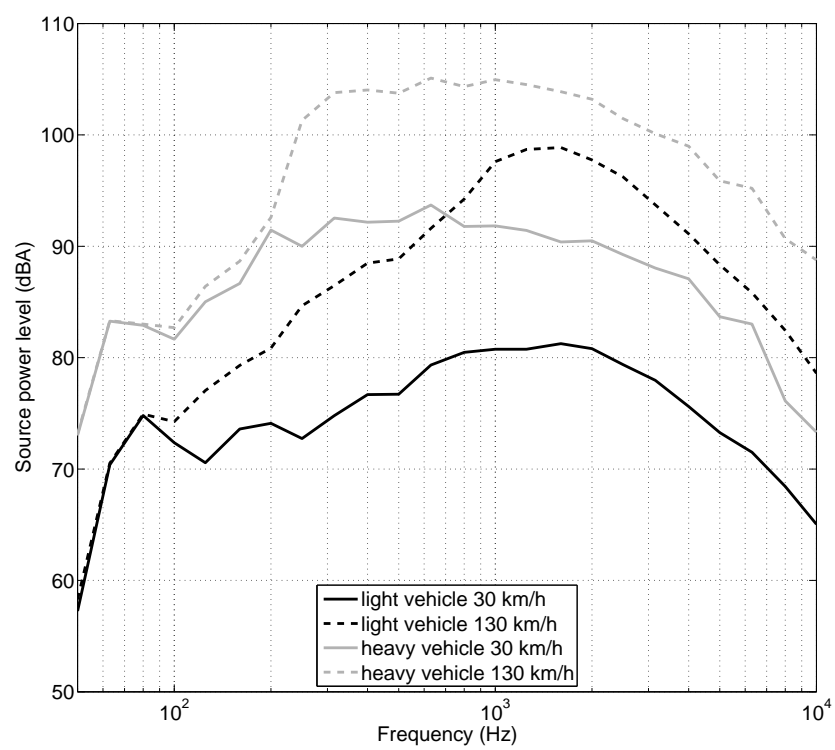


Figure 4

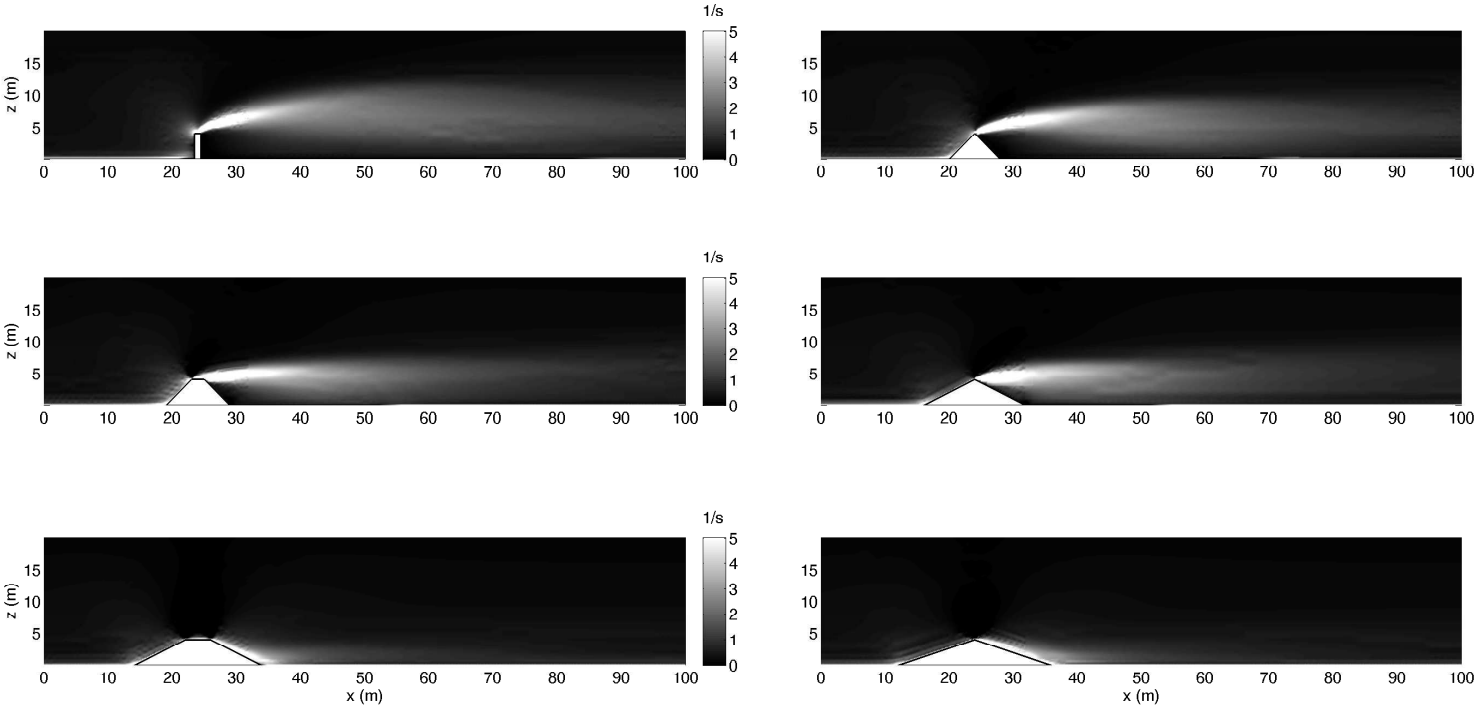


Figure 5

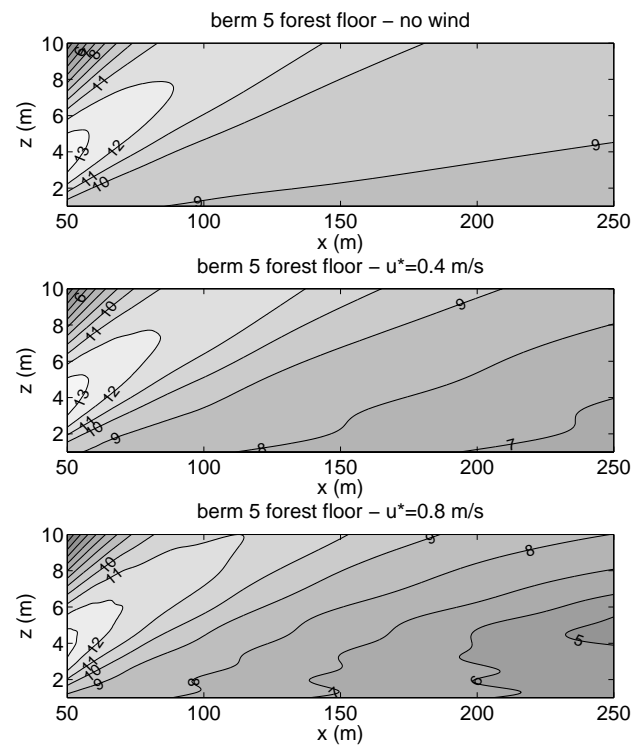
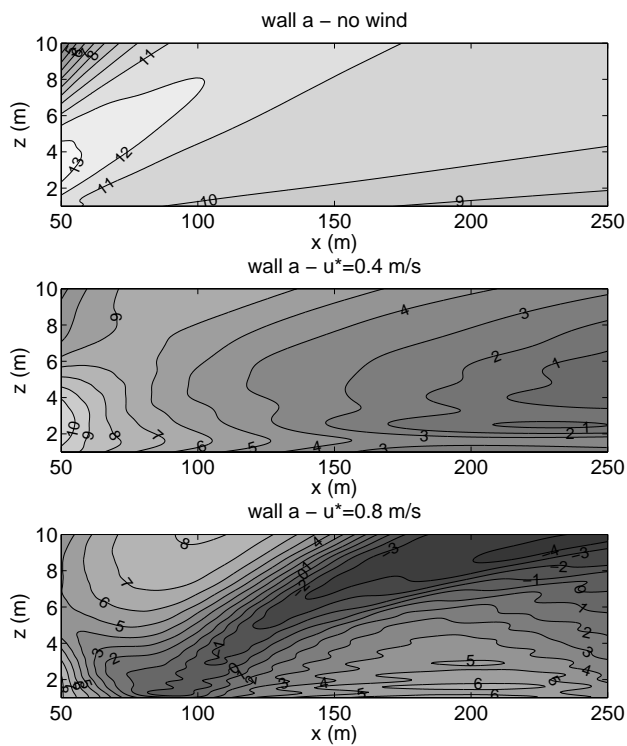


Figure 6

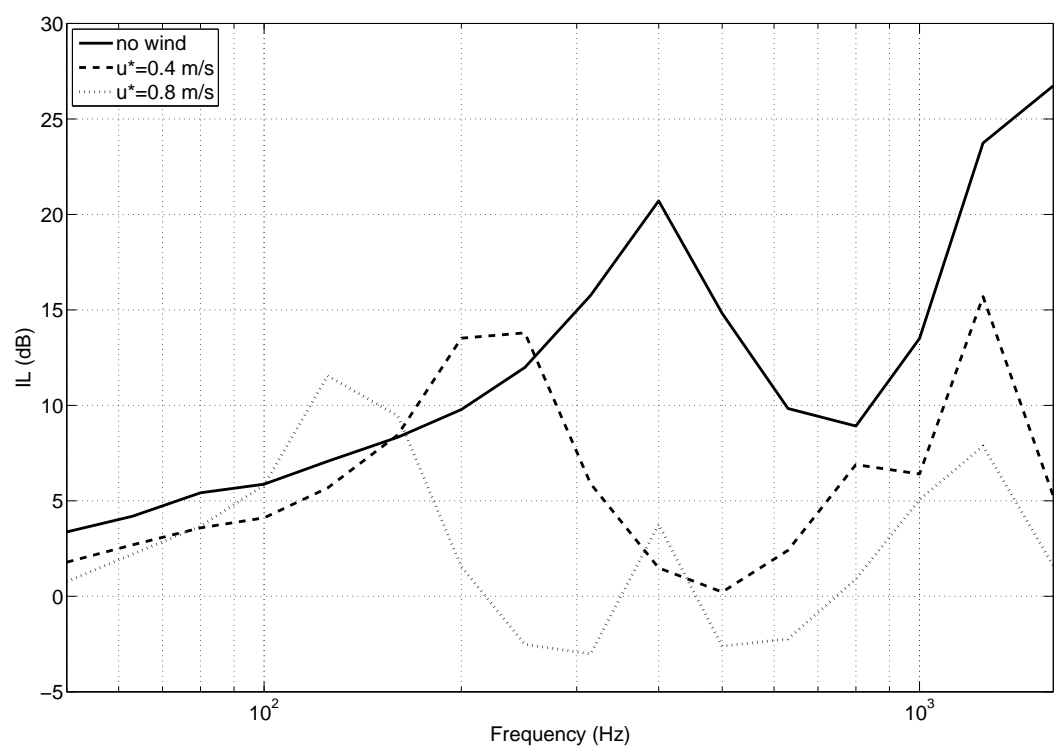
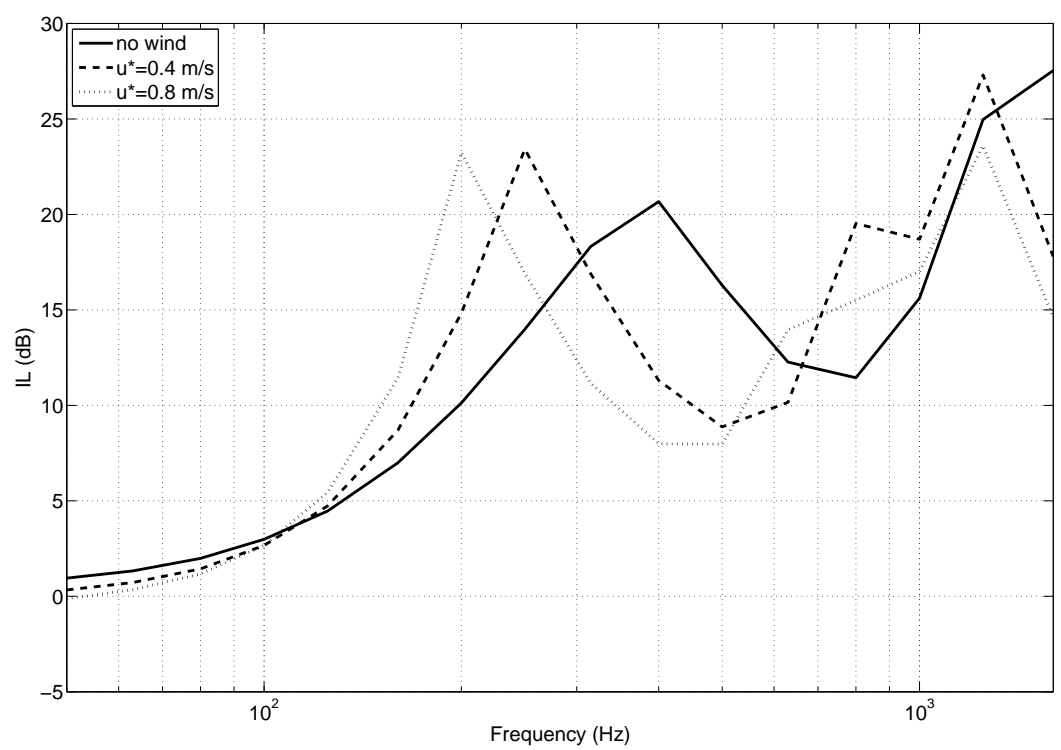


Figure 7



Acknowledgments

The research presented in this paper was partly funded by the European Community's Seventh Framework Programme (FP7/2007-2013) under grant agreement n° 234306, collaborative project HOSANNA.